

1 Non-linear transfer characteristics of stimulation and recording 2 hardware account for spurious low-frequency artifacts during 3 amplitude modulated transcranial alternating current stimula- 4 tion (AM-tACS)

5 Florian H. Kasten^{1,2}, Ehsan Negahbani³, Flavio Fröhlich^{3,4,5,6,7,8}, Christoph S. Herrmann^{1,2,9,*}

6 ¹Experimental Psychology Lab, Department of Psychology, European Medical School, Cluster for Ex-
7 cellence “Hearing for All”, Carl von Ossietzky University, Oldenburg, Germany

8 ²Neuroimaging Unit, European Medical School, Carl von Ossietzky University, Oldenburg, Germany

9 ³Department of Psychiatry, University of North Carolina, Chapel Hill, NC, USA

10 ⁴Department of Cell Biology and Physiology, University of North Carolina, Chapel Hill, NC, USA

11 ⁵Department of Biomedical Engineering, University of North Carolina, Chapel Hill, NC, USA

12 ⁶Neuroscience Center, University of North Carolina, Chapel Hill, NC, USA

13 ⁷Department of Neurology, University of North Carolina, Chapel Hill, NC, USA

14 ⁸Carolina Center for Neurostimulation, University of North Carolina, Chapel Hill, NC, USA

15 ⁹Research Center Neurosensory Science, Carl von Ossietzky University, Oldenburg, Germany

16
17 *Corresponding author: Christoph S. Herrmann, Experimental Psychology Lab, Carl von Ossi-
18 etzky University, Ammerländer Heerstr. 114 – 118, 26129, Oldenburg, Germany. chris-
19 toph.herrmann@uni-oldenburg.de, phone: +49 441 798 4936

20 21 **Abstract**

22 **Background:** Amplitude modulated transcranial alternating current stimulation (AM-tACS) has
23 been recently proposed as a possible solution to overcome the pronounced stimulation artifact
24 encountered when recording brain activity during tACS. In theory, AM-tACS does not entail
25 power at its modulating frequency, thus avoiding the problem of spectral overlap between brain
26 signal of interest and stimulation artifact. However, the current study demonstrates how weak
27 non-linear transfer characteristics inherent in stimulation and recording hardware can reintro-
28 duce spurious artifacts at the modulation frequency.

29 **Method:** The input-output transfer functions (TFs) of different stimulation setups were meas-
30 ured. The setups included basic recordings of signal-generator and stimulator outputs as well
31 as M/EEG phantom measurements. 6th-degree polynomial regression models were fitted to
32 model the input-output TFs of each setup. The resulting TF models were applied to digitally
33 generated AM-tACS signals to predict the location of spurious artifacts in the spectrum.

Kasten et al., 2018

Spurious low-frequency artifacts of AM-tACS

34 **Results:** All four setups measured for the study exhibited low-frequency artifacts at the mod-
35 ulation frequency and its harmonics when recording AM-tACS. Fitted TF models showed non-
36 linear contributions significantly different from zero (all $p < .05$) and successfully predicted the
37 frequency of artifacts observed in AM-signal recordings.

38 **Conclusions:** Our results suggest that even weak non-linearities of stimulation and recording
39 hardware can lead to spurious artifacts at the modulation frequency and its harmonics. Thus,
40 findings emphasize the need for more linear stimulation devices for AM-tACS and careful anal-
41 ysis procedures taking into account these low-frequency artifacts.

42

43 **Abstract: 232 words, Manuscript: 3986 words (including figure captions)**

44

45 **Keywords:** amplitude modulated transcranial alternating current stimulation (AM-tACS), MEG,
46 EEG, artifact, tACS, stimulation hardware.

47 **1 Introduction**

48 Transcranial alternating current stimulation (tACS) is receiving growing popularity as a tool to
49 interfere with endogenous brain oscillations in a frequency specific manner [1–5], allowing to
50 study causal relationships between these oscillations and cognitive functions [6,7]. Further, its
51 use might offer promising new pathways for therapeutic applications to treat neurological or
52 psychiatric disorders associated with dysfunctional neuronal oscillations [8–11].

53 While mechanisms of tACS have been studied in animals [1,5,12,13] and using computational
54 modelling [4,13,14], the investigation of tACS effects in human subjects has so far mostly been
55 studied behaviorally [15–17], by measuring BOLD response [18–20], or by tracking outlasting
56 effects in M/EEG signals [4,21–25]. Due to a strong electro-magnetic artifact, which spectrally
57 overlaps with the brain oscillation under investigation, online measurements of tACS effects in
58 M/EEG is challenging. However, uncovering these online effects is crucial as the aforemen-
59 tioned approaches can only provide limited, indirect insights to the mechanisms of action dur-
60 ing tACS in humans. In addition, online monitoring of physiological signals during stimulation
61 may enable closed-loop applications that can provide potentially more powerful, individually
62 tailored, adaptive stimulation protocols [26]. Some authors applied artifact suppression tech-
63 niques such as template subtraction [3,27,28] or spatial filtering [29,30] to recover brain signals
64 obtained during concurrent tACS-M/EEG. However, these approaches are computationally
65 costly, and therefore i.e. difficult to implement in closed-loop protocols. Further, their applica-
66 tion is limited as they fail to completely suppress the artifact and analysis approaches must be
67 limited to robust procedures to avoid false conclusions about stimulation effects [31–33].

68 As a solution to these issues, amplitude modulated tACS (AM-tACS), using a high frequency
69 carrier signal which is modulated in amplitude by a lower frequency modulation signal, chosen
70 to match the targeted brain oscillation has been proposed [34]. Amplitude modulated signals
71 contain spectral power at the frequency of the carrier signal (f_c ; and two sidebands at $f_c \pm f_m$;
72 modulation frequency), but no power at f_m itself (see **Figure 1** for an illustration). Conse-
73 quently, the tACS artifact would be shifted into higher frequencies, elegantly avoiding spectral
74 overlap with the targeted brain oscillation. However, more recently low-frequency artifacts at

75 f_m have been reported in sensor-level MEG recordings during AM-tACS [35]. These artifacts
76 required the application of advanced artifact suppression algorithms [35]. Although the authors
77 of that study explained these artifacts by non-linear characteristics of the digital-analog con-
78 version, a detailed investigation into these low-frequency artifacts arising during AM-tACS and
79 how these emerge has not yet been provided. In fact, the process of stimulation on the one
80 side and signal recording on the other side involves at least one step of digital-analog (gener-
81 ating a stimulation signal) and one step of analog-digital conversion (sampling brain signal plus
82 stimulation artifact). The linearity of these conversions, however, is naturally limited by proper-
83 ties of the hardware in use [36]. To further complicate the situation, the amplification involved
84 in the recording process using M/EEG can be another potential source of nonlinearity. The
85 amplitudes usually applied in tACS can potentially cause signals/artifacts, beyond the dynamic
86 range where the measurement devices exhibit linear transfer characteristics [37]. In general
87 all electronic components, including those that are usually idealized as being linear (i.e. resis-
88 tors), exhibit some degree of non-linearity in reality, especially when operating under extreme
89 conditions [38].
90 To shed more light on the effects of non-linearity of stimulation and recording hardware on AM-
91 tACS signals, input-output transfer functions (TFs) of different AM-tACS setups were estimated
92 and evaluated with respect to their performance in predicting low-frequency artifacts of AM-
93 tACS¹.

94 **2 Materials & Methods**

95 In order to characterize non-linearities inherent in different tACS setups, the transfer functions
96 (TFs) relating input-output amplitudes of four different tACS setups, with increasing complexity,
97 were recorded and modeled by polynomial regression models. Additionally, AM-tACS signals
98 were recorded to demonstrate the presence of low-frequency artifacts. TF models were applied
99 to digital AM-signals to predict output spectra of the physical recordings. The following four
100 setups were evaluated. No human or animal subjects were involved in the experiment.

¹ In contrast to the frequency-domain definition of TFs commonly used in linear-system analysis, here TF refers to the input-output amplitude relation of a probe signal.

101 **2.1 Test Setups**

102 **2.1.1 Basic DAC recording**

103 For the first, basic setup, a digital/analog-analog/digital converter (DAC; NiUSB-6251, National
104 Instruments, Austin, TX, USA) recorded its own output signal. The signal was digitally gener-
105 ated using Matlab 2016a (The MathWorks Inc., Natick, MA, USA) and streamed to the DAC
106 via the Data Acquisition Toolbox. The signal was generated and recorded at a rate of 10 kHz
107 (**Figure 1A**).

108 **2.1.2 DAC & tACS stimulator**

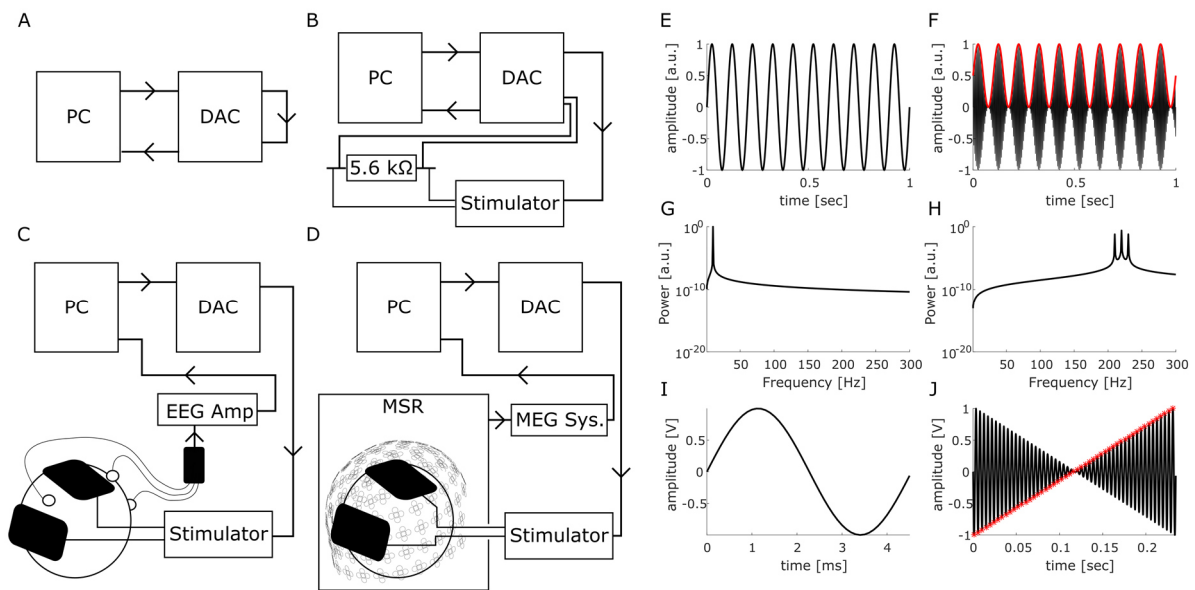
109 In the second setup the DAC was connected to the remote input of a battery-driven constant
110 current stimulator (DC Stimulator Plus, Neuroconn, Illmenau, Germany). Stimulation was ad-
111 ministered to a 5.6 k Ω resistor. The signal was recorded from both ends of the resistor using
112 the DAC (**Figure 1B**).

113 **2.1.3 DAC & tACS recorded from phantom using EEG**

114 In the third setup the DC Stimulator was connected to two surface conductive rubber electrodes
115 attached to a melon serving as a phantom head. Electrodes were attached using an electrically
116 conductive, adhesive paste (ten20, Weaver & Co., Aurora, CO, USA). The signal was recorded
117 from an active Ag/AgCl EEG electrode (ActiCap, Brain Products, Gilching, Germany), placed
118 between the tACS electrodes. Two additional electrodes were attached to the phantom to
119 serve as reference and ground for the recording (positions were chosen to mimic a nose-ref-
120 erence and a ground placed on the forehead). The signal was generated by the DAC at a rate
121 of 10 kHz and recorded at 10 kHz using a 24-bit ActiChamp amplifier (Brain Products, Gilching,
122 Germany). EEG and stimulation electrode impedances were kept below 10 k Ω (**Figure 1C**).

123 **2.1.4 DAC & tACS recorded from phantom using MEG**

124 Finally, the phantom was recorded using a 306-channel whole-head MEG system (Elekta Neu-
125 romag Triux, Elekta Oy, Helsinki, Finland) located inside a magnetically shielded room (MSR;
126 Vacuumschmelze, Hanau, Germany). Signals were recorded without internal active shielding



127

128 **Figure 1: Experimental setups and signals.** (A-D) Schematic representations of the evaluated setups. For details
129 refer to the “**Test setups**” section in the manuscript. DAC: Digital-Analog converter. MSR: Magnetically shielded-
130 room. Arrows indicate the direction of signal flow (E,F) Time domain representations of a low-frequency sine-wave
131 classically used for tACS (E) and an amplitude modulated sine wave with a carrier frequency of 220 Hz modulated
132 at 10 Hz (F). Red curve depicts the 10 Hz envelope of the signal. (G,H) Frequency-domain representations of the
133 tACS signals. While the 10 Hz sine wave exhibits its power at 10 Hz (G), the amplitude modulated signal only
134 exhibits power at the carrier frequency and two side-bands, but no power at the modulation frequency (F). (I) Probe
135 stimulus for measuring the setups transfer curves was a 220 Hz single-cycle sine wave. Probe stimuli of different
136 amplitude were concatenated to a sweep (J). Red asterisks mark points that were extracted as V_{out} measure. To
137 enhance visibility of the general concept, a sweep consisting of 51 probes is displayed here. For the actual meas-
138 urements of the TFs 10 sweeps with 10001 probes were used.

139 at a rate of 1 kHz and online filtered between 0.3 and 330 Hz. The stimulation signal was gated
140 into the MSR via the MRI-extension kit of the DC stimulator (Neuroconn, Illmenau, Germany;
141 **Figure 1D**).

142 2.2 Transfer function and AM-tACS measurements

143 A probe stimulus consisting of a one cycle sine wave at 220 Hz was used to obtain measure-
144 ments of each setups transfer function (TF). 10001 probes of linearly spaced amplitudes (V_{in}),
145 ranging from -10 V to 10 V for the first setup, from -0.75 V to 0.75 V for the second and third
146 setup, and from -0.5 V to 0.5 V for the MEG setup, were concatenated to a sweep stimulus
147 with a total duration of approximately 45 sec. (see **Figure 1I-J** for a schematic visualization).

148 Amplitudes had to be adjusted for setups involving the DC stimulator to account for higher
149 output voltages due to the 2 mA per V voltage-to-current conversion of the remote input. The
150 chosen input voltages correspond to a maximum output of 3 mA peak-to-peak amplitude of the
151 DC stimulator (a maximum current of 2 mA was chosen for the MEG setup to avoid saturation
152 and flux trapping of MEG sensors). Ten consecutive sweeps were applied and recorded for
153 each setup. In order to evaluate how well the obtained TF can predict artifacts in the spectrum
154 of AM-tACS, AM-signals with $f_c = 220$ Hz and $f_m = 10$ Hz, 11 Hz, and 23 Hz at different ampli-
155 tudes (100%, 66.7%, 33.4% and 16.16% of the maximum range applied during the TF record-
156 ing) were generated. Amplitudes were chosen to produce output currents of 3 mA, 2 mA, 1
157 mA, and 0.5 mA when using the DC-Stimulator (2 mA, 1.3 mA, 0.66 mA, 0.33 mA for the MEG
158 setup). AM-signals were computed based on the following equation:

$$159 \quad AM_{Signal}(t) = a_{stim} \left(\left(\frac{\sin(2\pi * f_m * t)}{2} + \frac{1}{2} \right) * \sin(2\pi * f_c * t) \right), \quad (1)$$

160 where a_{stim} is the stimulation amplitude, f_m is the modulation frequency and f_c is the carrier
161 frequency. Each signal was generated and recorded with 60 repetitions to increase signal-to-
162 noise ratios.

163 2.3 Data Analysis

164 Data analysis was performed using Matlab 2016a (The MathWorks Inc., Natick, MA, USA).
165 The fieldtrip toolbox [39] was used to import and segment M/EEG recordings. All scripts and
166 underlying datasets are available online (<https://osf.io/czb3d/>).

167 2.3.1 Data processing and transfer function estimation

168 The recorded sweeps were epoched into segments containing single cycles of the sine-waves
169 used as probes. All Segments were baseline corrected and the peak-amplitude (V_{out}) of each
170 epoch was extracted by identifying the minimum (for $V_{in} < 0$) or maximum values (for $V_{in} \geq 0$)
171 within each segment. A 6th-degree polynomial regression model was fitted to each repetition
172 of the sweep to predict V_{out} (recorded peak amplitudes) as a function of V_{in} (generated peak
173 amplitudes) using a least-square approach:

$$174 \quad \widehat{V}_{out} = f(V_{in}), \quad (2)$$

175 with:

$$176 \quad f(V_{in}) = \beta_6 * V_{in}^6 + \beta_5 * V_{in}^5 + \beta_4 * V_{in}^4 + \beta_3 * V_{in}^3 + \beta_2 * V_{in}^2 + \beta_1 * V_{in} + \beta_0 \quad (3)$$

177 The fitting procedure was performed separately for each sweep to obtain measures of variance
178 for each of the coefficients. Coefficients were averaged subsequently and the resulting function
179 was used to model each systems TF. R^2 -values were calculated as measures for goodness of
180 fit.

181 In order to evaluate the performance of the TF models in predicting low-frequency AM-tACS
182 artifacts of the setups, the digitally generated AM-tACS signals were fed through the TF mod-
183 els. Subsequently, the predicted output signals were compared to the AM-tACS recordings
184 acquired for each setup. To this end, power spectra of the original digital, the predicted and
185 the recorded AM-signals were computed. The resulting power spectra of the AM-signals were
186 averaged over the 60 repetitions. For the MEG recording, results are presented for an exem-
187 plary parieto-occipital gradiometer sensor (MEG2113).

188 **2.3.2 Identification of low-frequency artifacts**

189 To identify systematic artifacts in the spectrum of the AM-signal in the noisy recordings, the
190 averaged power spectra were scanned for artifacts within a range from 2 Hz to 301 Hz. Artifacts
191 were defined as the power at a given frequency being altered by at least 5% as compared to
192 the mean power of the two neighboring frequencies. The identified artifacts were statistically
193 compared to the power in the two neighboring frequencies using student's t-tests. Bonferroni-
194 correction was applied to strictly account for multiple comparisons.

195 **2.3.3 Simulation**

196 To evaluate the effect of each non-linear term in the TF models on the output signal, a simu-
197 lation was carried out. To this end an amplitude modulated signal with $f_c = 220 \text{ Hz}$ and $f_m =$
198 10 Hz was evaluated by simplified TFs where all coefficients were set to zero except for the
199 linear and one additional non-linear term which were set to one in each run. This procedure

200 leads to exaggerated output spectra that do not realistically resemble the recorded TFs. How-
201 ever, they are well suited to illustrate the spectral artifacts arising from each of the non-linear
202 terms.

203 In addition to the AM-signal, we generated a temporal interference (TI) signal that was recently
204 proposed as a tool to non-invasively stimulate deep structures of the brain [40]. TI stimulation
205 consists of two externally applied, high frequency sine waves of slightly differing frequencies
206 that result in an AM-signal where their electric fields overlap. Since the generation of this AM-
207 signal is mathematically slightly different as compared to the other AM-tACS approach, this
208 signal was separately modelled for two stimulation signals based on the following equation:

$$209 \quad TI_{Signal}(t) = a_{Stim} * \frac{(\sin(2\pi*f_1*t) + \sin(2\pi*f_2*t))}{2}, \quad (4)$$

210 with $f_1 = 200 \text{ Hz}$ and $f_2 = 210 \text{ Hz}$. The overlap of these two frequencies results in an amplitude
211 modulation at 10 Hz.

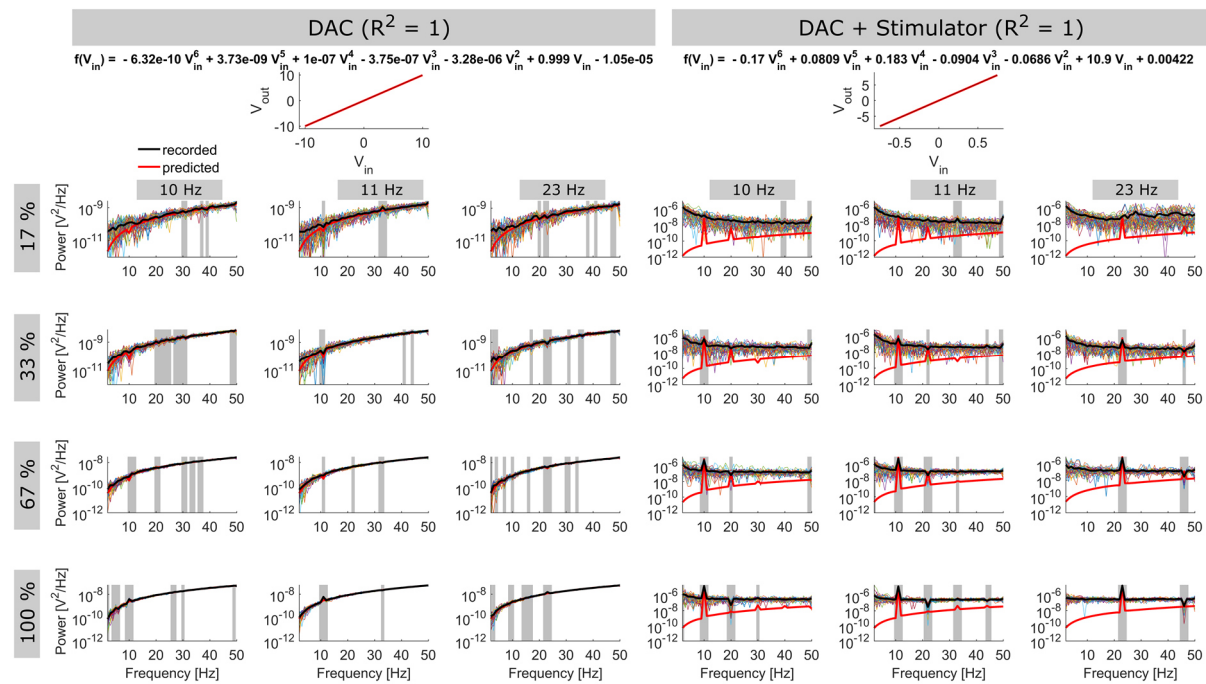
212 **3 Results**

213 **3.1 Systematic artifacts at modulation frequency of AM-tACS and harmonics**

214 Analysis of the AM-tACS recordings identified systematic artifacts at the modulation frequency
215 and its harmonics that statistically differed from power at neighboring frequencies in all setups
216 (all $p < .05$; **Figure 2** and **3**). Notably, these artifacts were comparatively small, albeit still sig-
217 nificant at larger amplitudes, when the DAC measured its own output without any further de-
218 vices in the setup (**Figure 2 left**). When the complexity of the setup was increased, more and
219 stronger artifacts were observed (**Figure 2 right, Figure 3**). The number and size of artifacts
220 also tended to increase with stronger stimulation amplitudes. **Figures 2** and **3** depict lower
221 frequency spectra (1 Hz – 50 Hz) for all setups and frequency-amplitude combinations tested.

222 **3.2 Setups exhibit non-linear transfer characteristics**

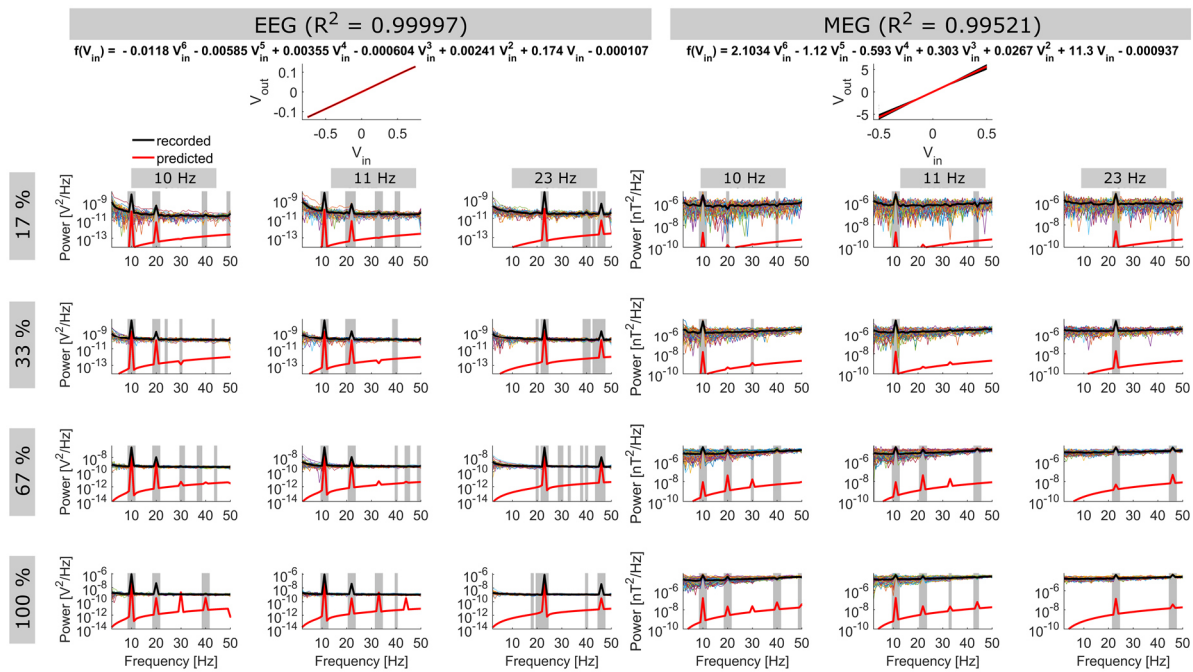
223 To obtain a model of each setups TF, 6th-degree polynomial regression models were fitted to
224 the input-output amplitudes of the probe stimuli. All setups tested in this study exhibited coef-
225 ficients of the non-linear terms of the fitted TFs significantly differing from zero.



226

227 **Figure 2: Transfer functions (top row) and spectra (lower rows) of setups of the DAC and Stimulator setup.**

228 TFs (top) show recorded probe stimulus amplitudes in relation to their input amplitudes (V_{out}/V_{in} ; black dots), as
 229 well as the course of the TF model (red line). The corresponding function is displayed in the title. Spectra show
 230 average power at each frequency in the different AM-recordings (black line). Thin colored lines show power spectra
 231 for each of the 60 repetitions. Red line shows the spectrum predicted by evaluating the digital AM-signal by the
 232 estimated TF of the setup. Grey areas indicate frequencies significantly differing in power compared to the two
 233 neighboring frequencies ($p < .05$, bonferroni corrected). Please note the different scaling of the power spectra. To
 234 enhance visibility, spectra are limited to the frequency range between 1 Hz and 50 Hz. Please refer to the **Supple-**
 235 **mentary Materials** for an alternative version of the figure, covering the full frequency range between 1 and 300 Hz.
 236 In setups 1, 2, and 4 all model coefficients significantly differed from zero (all $p < .004$; bonfer-
 237 roni corrected). For the EEG setup, coefficients β_2 ($p < .02$), β_5 ($p < .004$) and β_6 ($p < .007$)
 238 significantly differed from zero. Results are summarized in **Table 1**. High goodness of fit values
 239 were achieved for all setups under investigation ($R^2 > .99$), indicating that the polynomial func-
 240 tions provide powerful models to describe the input-output characteristics of the setups. Im-
 241 portantly, the non-linearities found during this analysis are subtle compared to the contribution
 242 of the linear terms in each TF. This leads to the impression of linearity when visually inspecting
 243 each setups TF (**Figure 2,3 top panel**). However, as it will be shown in the following, these
 244 small deviations from linearity are sufficient to cause the low frequency artifacts observed dur-
 245 ing the AM-tACS recordings.



246

247 **Figure 3: Transfer functions (top row) and spectra (lower rows) of the EEG and MEG setup.** TFs (top) show
 248 recorded probe stimulus amplitudes in relation to their input amplitudes (V_{out}/V_{in} ; black dots), as well as the course
 249 of the TF model (red line). The corresponding function is displayed in the title. Output values (V_{out}) for the MEG
 250 setup are expressed in nT. Spectra show average power at each frequency in the different AM-recordings (black
 251 line). Thin, colored lines show power spectra for each of the 60 repetitions. Red line shows the spectrum predicted
 252 by evaluating the digital AM-signal by the estimated TF of the setup. Grey areas indicate frequencies significantly
 253 differing in power compared to the two neighboring frequencies ($p < .05$, bonferroni-corrected). Please note the
 254 different scaling and units of the power spectra. To enhance visibility, spectra are limited to the frequency range
 255 between 1 Hz and 50 Hz. Please refer to the **Supplementary Materials** for an alternative version of the figure,
 256 covering the full frequency range between 1 and 300 Hz.

257 3.3 Transfer functions predict frequency of spurious artifacts

258 When applying the TF models to the digital AM-signals, the resulting spectra provide accurate
 259 predictions of the systematic low-frequency artifacts at f_m of the AM-signal and its lower har-
 260 monics in the recordings. For the first two setups, where the TF models' goodness of fit is
 261 equal to 1, the predicted spectra also capture the amplitudes low-frequency artifacts with rela-
 262 tively high accuracy (**Figure 2**). For the two later setups, however, the predicted spectrum
 263 apparently underestimates amplitudes of the artifacts (**Figure 3**). In summary, results suggest
 264 that the polynomial functions fitted to the data successfully captured the non-linear process
 265 leading to the low-frequency artifacts at f_m , although for the later setups, that exhibited more

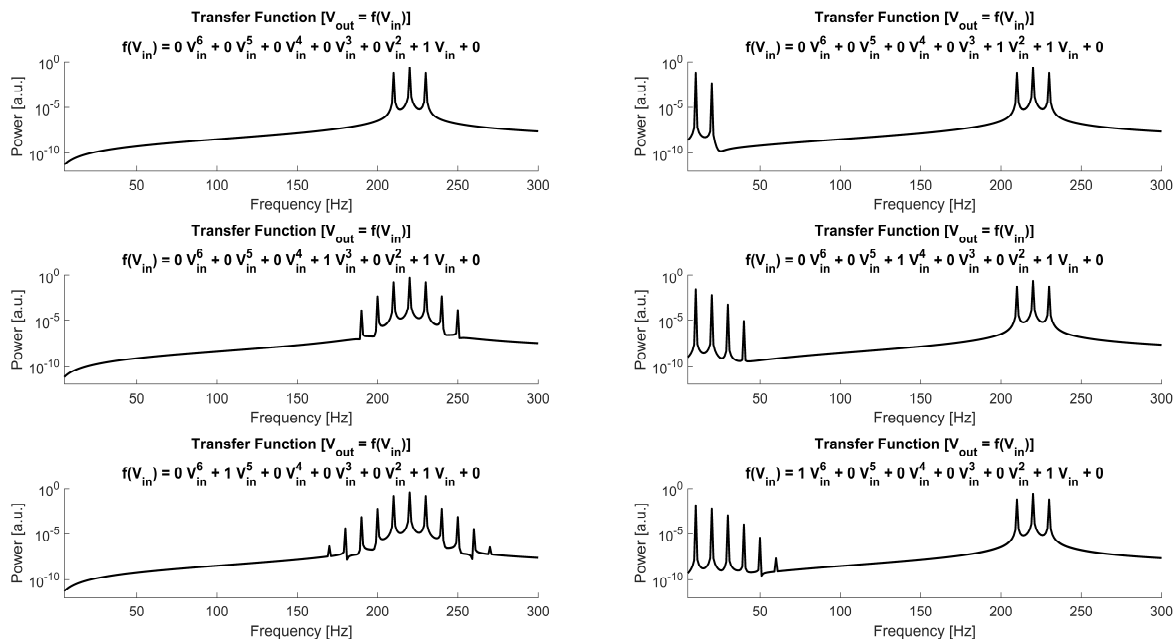
266 noise during the measurements, accuracy of the fits seems not sufficient to accurately predict
267 the artifacts amplitudes. In addition, it should be noted that the application of a TF to a pure
268 digital AM-signal can never completely capture the effects of the recording process that in-
269 volves measurement of noise and external interferences (i.e. line-noise).

270 **3.4 Simulating the isolated effect of non-linear TF-terms**

271 Based on the results presented so far, it was possible to characterize each the non-linearity of
272 each setup and to demonstrate that the estimated TF can be used to predict artifacts in the
273 recorded AM-signals. However, since the obtained TFs are rather complex, a simulation was
274 carried out to investigate the artifacts caused by each of the non-linear terms in isolation. The
275 spectra obtained from this simulation are depicted in **Figure 4**. While a solely linear TF does
276 not change the spectral content of the AM-signal at all (**Figure 4 top left**), polynomial terms
277 with odd exponents > 1 result in additional side bands around f_c of the AM-signal (**Figure 4**
278 **middle, bottom left**). In contrast, terms with even exponents induced artifacts at f_m and its
279 harmonics (**Figure 4 right column**). The higher the exponent of the polynomial terms the more
280 sidebands and higher harmonics are introduced to the spectrum, respectively. A separate
281 simulation for an AM-signal resulting from temporal interference [40] yielded a similar result
282 (**Supplementary Figure S3**).

283 **4 Discussion**

284 Amplitude modulated transcranial alternating current stimulation (AM-tACS) offers a promising
285 new approach to investigate online effects of tACS using physiological recordings. While in
286 theory AM-tACS should not exhibit artifacts within the frequency range of brain signals, the
287 current study demonstrates that non-linear transfer characteristics of stimulation and recording
288 hardware reintroduces such artifacts at the modulation frequency and its lower harmonics.
289 While these artifacts are likely too small to modulate brain activity themselves, they can poten-
290 tially be misinterpreted as stimulation effects on the brain if not considered during concurrent
291 recordings of brain activity during AM-tACS. Consequently, these recordings must not be con-



292

293 **Figure 4: Simulation results. (Left column)** Spectra resulting from evaluating the digital AM-signal using a sim-
 294 plified TF. A solely linear TF (**top left**) perfectly resembles the input spectrum. Setting the coefficient of an additional
 295 polynomial term with an odd-valued exponent to 1 resulted in additional side bands around f_c (**middle and bottom**
 296 **left**). In contrast, setting the coefficient of an additional polynomial term with an even-valued exponent to 1 resulted
 297 in artifacts at f_m and its harmonics (**right column**). The higher the exponent of the polynomial terms, the more side-
 298 bands/harmonic artifacts they introduced. The polynomial function applied to generate each spectrum is printed on
 299 top of each plot.

300 sidered artifact-free in the range of the modulation frequency. Rather, the extent of low-fre-
 301 quency artifacts has to be evaluated carefully and taken into account.

302 The setups evaluated for the current study have been build based on a limited set of hardware.
 303 Thus, the extent of non-linearity might differ for hardware combinations using other stimulator
 304 or recording systems. However, since all electronic components exhibit some degree of non-
 305 linearity [38], the general process underlying the generation of low-frequency AM-tACS arti-
 306 facts is potentially applicable to all setups. Only the size of these artifacts can differ depending
 307 on the (non-)linearity of the system. The current study provides a framework to measure and
 308 estimate a setups transfer characteristics and evaluate the strength of these low-frequency
 309 artifacts arising from its non-linearities. Interestingly, the DAC itself exhibited comparatively
 310 weak artifacts, while the more complex setups showed stronger artifacts at the modulation

311 frequency and several harmonics. This might indicate that the effect is driven by non-linearities
312 of the stimulator or recording hardware rather than the DAC as suggested by previous authors
313 [35].

314 To obtain a model of each setups transfer characteristics, polynomial regression models were
315 fitted to the probe-signal recordings. The degree of the models is a best guess to tradeoff
316 sufficient complexity to capture each setups nonlinearity, and simplicity to retain a straightfor-
317 ward, interpretable model. Unfortunately, traditional approaches for model selection, i.e. based
318 on adjusted R^2 or Akaike Information Criterion, that start from a simple intercept or a saturated
319 model, are not applicable to the data at hand, as the non-linearities observed in the setups are
320 very subtle. A simple linear model would already account for a huge proportion of the input-
321 output recordings variance. Adding additional higher degree terms to the model does not suf-
322 ficiently increase the explained variance to counteract the penalty implemented in most model
323 evaluation metrics. However, as seen in the simulated data only these terms account for the
324 low-frequency artifacts observed in the AM-tACS recordings.

325 Given that the low-frequency AM-tACS artifacts are several orders of magnitude smaller than
326 the artifact arising during classical tACS (or at the carrier frequency), they are potentially easier
327 to correct/suppress i.e. by applying beamforming [34,41] or temporal signal space separation
328 [35,42] in the MEG and independent or principal component analysis (ICA/PCA) in the EEG
329 [3]. However, the efficiency of these methods in the context of AM-tACS needs to be system-
330 atically investigated in future studies. The optimal solution to overcome the artifacts observed
331 here would be the optimization of stimulation and recording hardware with respect to their
332 linearity. Neither have tES devices currently available been purposefully designed to apply AM-
333 tACS, nor are recording systems for brain activity intended to record AM-signals at intensities
334 as observed during AM-tACS. Devices exhibiting more linear transfer characteristics as i.e.
335 observed for the DAC output in setup 1 would decrease the size of the artifacts compared to
336 the signal of interest such that its influence eventually becomes negligible. Until such devices
337 are available, careful analysis procedures have to be carried out, to ensure trustworthy results
338 from concurrent AM-tACS-M/EEG studies.

339 **5 Conflict of interest**

340 CH has filed a patent application on brain stimulation and received honoraria as editor from
341 Elsevier Publishers, Amsterdam. FF is the founder, chief scientific officer, and majority owner
342 of Pulvinar Neuro LLC. FK and EN declare no competing interests.

343 **6 Author contributions**

344 FK, EN, FF and CSH, conceived the study. FK collected and analyzed the data. All authors
345 wrote the manuscript.

346 **7 Acknowledgements**

347 This research was supported by the Neuroimaging Unit of the Carl von Ossietzky University
348 Oldenburg funded by grants from the German Research Foundation (3T MRI INST 184/152-1
349 FUGG and MEG INST 184/148-1 FUGG). Christoph S. Herrmann was supported by a grant
350 of the German Research Foundation (DFG, SPP, 1665 3353/8-2). This work was supported in
351 part by the National Institute of Mental Health of the National Institutes of Health under award
352 numbers R01MH111889 and R01MH101547 (PI: Flavio Frohlich). The content is solely the
353 responsibility of the authors and does not necessarily represent the official views of the Na-
354 tional Institutes of Health.

355 **8 References**

- 356 [1] Fröhlich F, McCormick DA. Endogenous Electric Fields May Guide Neocortical Network
357 Activity. *Neuron* 2010;67:129–43. doi:10.1016/j.neuron.2010.06.005.
- 358 [2] Herrmann CS, Rach S, Neuling T, Strüber D. Transcranial alternating current
359 stimulation: a review of the underlying mechanisms and modulation of cognitive
360 processes. *Front Hum Neurosci* 2013;7:1–13. doi:10.3389/fnhum.2013.00279.
- 361 [3] Helfrich RF, Schneider TR, Rach S, Trautmann-Lengsfeld SA, Engel AK, Herrmann CS.
362 Entrainment of Brain Oscillations by Transcranial Alternating Current Stimulation. *Curr*
363 *Biol* 2014;24:333–9. doi:10.1016/j.cub.2013.12.041.

- 364 [4] Zaehle T, Rach S, Herrmann CS. Transcranial Alternating Current Stimulation
365 Enhances Individual Alpha Activity in Human EEG. *PLoS One* 2010;5:13766.
366 doi:10.1371/journal.pone.0013766.
- 367 [5] Ozen S, Sirota A, Belluscio MA, Anastassiou CA, Stark E, Koch C, et al. Transcranial
368 Electric Stimulation Entraines Cortical Neuronal Populations in Rats. *J Neurosci*
369 2010;30:11476–85. doi:10.1523/JNEUROSCI.5252-09.2010.
- 370 [6] Herrmann CS, Strüber D, Helfrich RF, Engel AK. EEG oscillations: From correlation to
371 causality. *Int J Psychophysiol* 2016;103:12–21. doi:10.1016/j.ijpsycho.2015.02.003.
- 372 [7] Fröhlich F. Experiments and models of cortical oscillations as a target for noninvasive
373 brain stimulation. *Prog. Brain Res.*, vol. 222, 2015, p. 41–73.
374 doi:10.1016/bs.pbr.2015.07.025.
- 375 [8] Herrmann CS, Demiralp T. Human EEG gamma oscillations in neuropsychiatric
376 disorders. *Clin Neurophysiol* 2005;116:2719–33. doi:10.1016/j.clinph.2005.07.007.
- 377 [9] Uhlhaas PJ, Singer W. Neuronal Dynamics and Neuropsychiatric Disorders: Toward a
378 Translational Paradigm for Dysfunctional Large-Scale Networks. *Neuron* 2012;75:963–
379 80. doi:10.1016/j.neuron.2012.09.004.
- 380 [10] Uhlhaas PJ, Singer W. Neural Synchrony in Brain Disorders: Relevance for Cognitive
381 Dysfunctions and Pathophysiology. *Neuron* 2006;52:155–68.
382 doi:10.1016/j.neuron.2006.09.020.
- 383 [11] Brittain J-S, Probert-Smith P, Aziz TZ, Brown P. Tremor Suppression by Rhythmic
384 Transcranial Current Stimulation. *Curr Biol* 2013;23:436–40.
385 doi:10.1016/j.cub.2013.01.068.
- 386 [12] Kar K, Duijnhouwer J, Krekelberg B. Transcranial Alternating Current Stimulation
387 Attenuates Neuronal Adaptation. *J Neurosci* 2017;37:2325–35.
388 doi:10.1523/JNEUROSCI.2266-16.2016.

- 389 [13] Reato D, Rahman A, Bikson M, Parra LC. Low-Intensity Electrical Stimulation Affects
390 Network Dynamics by Modulating Population Rate and Spike Timing. *J Neurosci*
391 2010;30:15067–79. doi:10.1523/JNEUROSCI.2059-10.2010.
- 392 [14] Ali MM, Sellers KK, Frohlich F. Transcranial Alternating Current Stimulation Modulates
393 Large-Scale Cortical Network Activity by Network Resonance. *J Neurosci*
394 2013;33:11262–75. doi:10.1523/JNEUROSCI.5867-12.2013.
- 395 [15] Lustenberger C, Boyle MR, Foulser AA, Mellin JM, Fröhlich F. Functional role of frontal
396 alpha oscillations in creativity. *Cortex* 2015;67:74–82.
397 doi:10.1016/j.cortex.2015.03.012.
- 398 [16] Kar K, Krekelberg B. Transcranial Alternating Current Stimulation Attenuates Visual
399 Motion Adaptation. *J Neurosci* 2014;34:7334–40. doi:10.1523/JNEUROSCI.5248-
400 13.2014.
- 401 [17] Neuling T, Rach S, Wagner S, Wolters CH, Herrmann CS. Good vibrations: Oscillatory
402 phase shapes perception. *Neuroimage* 2012;63:771–8.
403 doi:10.1016/j.neuroimage.2012.07.024.
- 404 [18] Violante IR, Li LM, Carmichael DW, Lorenz R, Leech R, Hampshire A, et al. Externally
405 induced frontoparietal synchronization modulates network dynamics and enhances
406 working memory performance. *Elife* 2017;6. doi:10.7554/eLife.22001.
- 407 [19] Vosskuhl J, Huster RJ, Herrmann CS. BOLD signal effects of transcranial alternating
408 current stimulation (tACS) in the alpha range: A concurrent tACS-fMRI study.
409 *Neuroimage* 2015. doi:10.1016/j.neuroimage.2015.10.003.
- 410 [20] Cabral-Calderin Y, Williams KA, Opitz A, Dechent P, Wilke M. Transcranial alternating
411 current stimulation modulates spontaneous low frequency fluctuations as measured
412 with fMRI. *Neuroimage* 2016;141:88–107. doi:10.1016/j.neuroimage.2016.07.005.
- 413 [21] Neuling T, Rach S, Herrmann CS. Orchestrating neuronal networks: sustained after-
414 effects of transcranial alternating current stimulation depend upon brain states. *Front*

- 415 Hum Neurosci 2013;7:161. doi:10.3389/fnhum.2013.00161.
- 416 [22] Kasten FH, Dowsett J, Herrmann CS. Sustained Aftereffect of α -tACS Lasts Up to 70
417 min after Stimulation. Front Hum Neurosci 2016;10:1–9.
418 doi:10.3389/fnhum.2016.00245.
- 419 [23] Kasten FH, Herrmann CS. Transcranial Alternating Current Stimulation (tACS)
420 Enhances Mental Rotation Performance during and after Stimulation. Front Hum
421 Neurosci 2017;11:1–16. doi:10.3389/fnhum.2017.00002.
- 422 [24] Vossen A, Gross J, Thut G. Alpha Power Increase After Transcranial Alternating Current
423 Stimulation at Alpha Frequency (α -tACS) Reflects Plastic Changes Rather Than
424 Entrainment. Brain Stimul 2015;8:499–508. doi:10.1016/j.brs.2014.12.004.
- 425 [25] Veniero D, Vossen A, Gross J, Thut G. Lasting EEG/MEG Aftereffects of Rhythmic
426 Transcranial Brain Stimulation: Level of Control Over Oscillatory Network Activity. Front
427 Cell Neurosci 2015;9:477. doi:10.3389/fncel.2015.00477.
- 428 [26] Bergmann TO, Karabanov A, Hartwigsen G, Thielscher A, Siebner HR. Combining non-
429 invasive transcranial brain stimulation with neuroimaging and electrophysiology: Current
430 approaches and future perspectives. Neuroimage 2016;140:4–19.
431 doi:10.1016/j.neuroimage.2016.02.012.
- 432 [27] Voss U, Holzmann R, Hobson A, Paulus W, Koppehele-Gossel J, Klimke A, et al.
433 Induction of self awareness in dreams through frontal low current stimulation of gamma
434 activity. Nat Neurosci 2014;17:810–2. doi:10.1038/nn.3719.
- 435 [28] Dowsett J, Herrmann CS. Transcranial Alternating Current Stimulation with Sawtooth
436 Waves: Simultaneous Stimulation and EEG Recording. Front Hum Neurosci 2016;10:1–
437 10. doi:10.3389/fnhum.2016.00135.
- 438 [29] Neuling T, Ruhnau P, Fuscà M, Demarchi G, Herrmann CS, Weisz N. Friends, not foes:
439 Magnetoencephalography as a tool to uncover brain dynamics during transcranial
440 alternating current stimulation. Neuroimage 2015;118:406–13.

- 441 doi:10.1016/j.neuroimage.2015.06.026.
- 442 [30] Ruhnau P, Neuling T, Fuscá M, Herrmann CS, Demarchi G, Weisz N. Eyes wide shut:
443 Transcranial alternating current stimulation drives alpha rhythm in a state dependent
444 manner. *Sci Rep* 2016;6:27138. doi:10.1038/srep27138.
- 445 [31] Noury N, Hipp JF, Siegel M. Physiological processes non-linearly affect
446 electrophysiological recordings during transcranial electric stimulation. *Neuroimage*
447 2016;140:99–109. doi:10.1016/j.neuroimage.2016.03.065.
- 448 [32] Noury N, Siegel M. Phase properties of transcranial electrical stimulation artifacts in
449 electrophysiological recordings. *Neuroimage* 2017.
450 doi:10.1016/j.neuroimage.2017.07.010.
- 451 [33] Neuling T, Ruhnau P, Weisz N, Herrmann CS, Demarchi G. Faith and oscillations
452 recovered: On analyzing EEG/MEG signals during tACS. *Neuroimage* 2017;147:960–
453 3. doi:10.1016/j.neuroimage.2016.11.022.
- 454 [34] Witkowski M, Garcia-Cossio E, Chander BS, Braun C, Birbaumer N, Robinson SE, et
455 al. Mapping entrained brain oscillations during transcranial alternating current
456 stimulation (tACS). *Neuroimage* 2015. doi:10.1016/j.neuroimage.2015.10.024.
- 457 [35] Minami S, Amano K. Illusory Jitter Perceived at the Frequency of Alpha Oscillations.
458 *Curr Biol* 2017;27:2344–2351.e4. doi:10.1016/j.cub.2017.06.033.
- 459 [36] Vargha B, Schoukens J, Rolain Y. Static nonlinearity testing of digital-to-analog
460 converters. *IEEE Trans Instrum Meas* 2001;50:1283–8. doi:10.1109/19.963198.
- 461 [37] Cooper, R., Osselton, J. W., & Shaw JC. *Recording Systems. EEG Technol.* 2nd ed.,
462 London: Butterworths & Co. LTD; 1974, p. 47–79. doi:10.1016/B978-0-407-16001-
463 9.50001-8.
- 464 [38] Maas, Stephen A. *Nonlinear Microwave and RF Circuits.* 2nd ed. Boston: Artec House;
465 2003.

- 466 [39] Oostenveld R, Fries P, Maris E, Schoffelen JM. FieldTrip: Open source software for
 467 advanced analysis of MEG, EEG, and invasive electrophysiological data. *Comput Intell*
 468 *Neurosci* 2011;2011:1–9. doi:10.1155/2011/156869.
- 469 [40] Grossman N, Bono D, Dedic N, Kodandaramaiah SB, Rudenko A, Suk H-J, et al.
 470 Noninvasive Deep Brain Stimulation via Temporally Interfering Electric Fields. *Cell*
 471 2017;169:1029–1041.e16. doi:10.1016/j.cell.2017.05.024.
- 472 [41] Chander BS, Witkowski M, Braun C, Robinson SE, Born J, Cohen LG, et al. tACS Phase
 473 Locking of Frontal Midline Theta Oscillations Disrupts Working Memory Performance.
 474 *Front Cell Neurosci* 2016;10:1–10. doi:10.3389/fncel.2016.00120.
- 475 [42] Taulu S, Simola J, Kajola M. Applications of the signal space separation method. *IEEE*
 476 *Trans Signal Process* 2005;53:3359–72. doi:10.1109/TSP.2005.853302.

477 9 Tables

478 **Table 1:** Transfer function coefficients tested for deviation from zero. Coefficients of the 10
 479 polynomial functions fitted for each setups TF recordings were tested against zero using stu-
 480 dent's t-test (two-sided, bonferroni corrected). Mean and standard deviation are shown for
 481 each coefficient.

	<i>Mean</i>	<i>Std.</i>	<i>df</i>	<i>T</i>	<i>p</i>
<i>DAC</i>					
β_0	-1.05e-05	4.80e-06	9	-6.92	< .001*
β_1	0.9988	1.86e-05	9	> 100	< .001*
β_2	-3.28e-06	7.02e-07	9	-14.79	< .001*
β_3	-3.75e-07	7.16e-08	9	-16.56	< .001*
β_4	9.99e-08	2.31e-08	9	13.69	< .001*
β_5	3.73e-09	5.77e-10	9	20.41	< .001*
β_6	-6.32e-10	1.72e-10	9	-11.63	< .001*
<i>DAC + Stimulator</i>					
β_0	0.0042	0.0009	9	15.37	< .001*
β_1	10.8640	0.0123	9	> 100	< .001*
β_2	-0.0686	0.0153	9	-14.14	< .001*
β_3	-0.0904	0.0324	9	-8.83	< .001*
β_4	0.1838	0.0606	9	9.54	< .001*

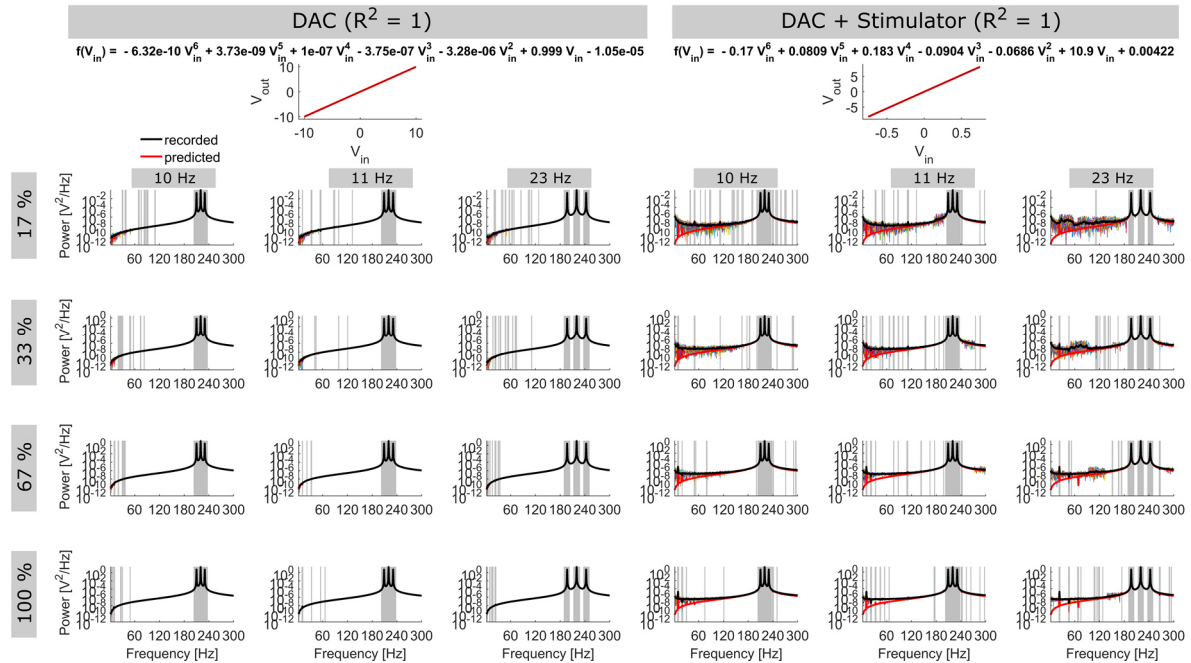
β_5	0.0809	0.0484	9	5.28	< .001*
β_6	-0.1702	0.0712	9	-7.56	< .001*
EEG					
β_0	-0.0001	0.0001	9	-5.27	< .001*
β_1	0.1736	0.0007	9	> 100	< .001*
β_2	0.0024	0.0017	9	4.44	.002*
β_3	-0.0006	0.0024	9	-0.81	.44
β_4	0.0035	0.0069	9	1.64	.14
β_5	-0.0058	0.0035	9	-5.30	< .001*
β_6	-0.0118	0.0078	9	-4.80	.001*
MEG					
β_0	-0.0009	0.0002	9	-16.35	< .001*
β_1	11.3235	0.0576	9	> 100	< .001*
β_2	0.0267	0.0121	9	6.97	< .001*
β_3	0.3033	0.0393	9	24.41	< .001*
β_4	-0.5931	0.1532	9	-12.24	< .001*
β_5	-1.1228	0.2065	9	-17.19	< .001*
β_6	2.1034	0.5192	9	12.81	< .001*

482

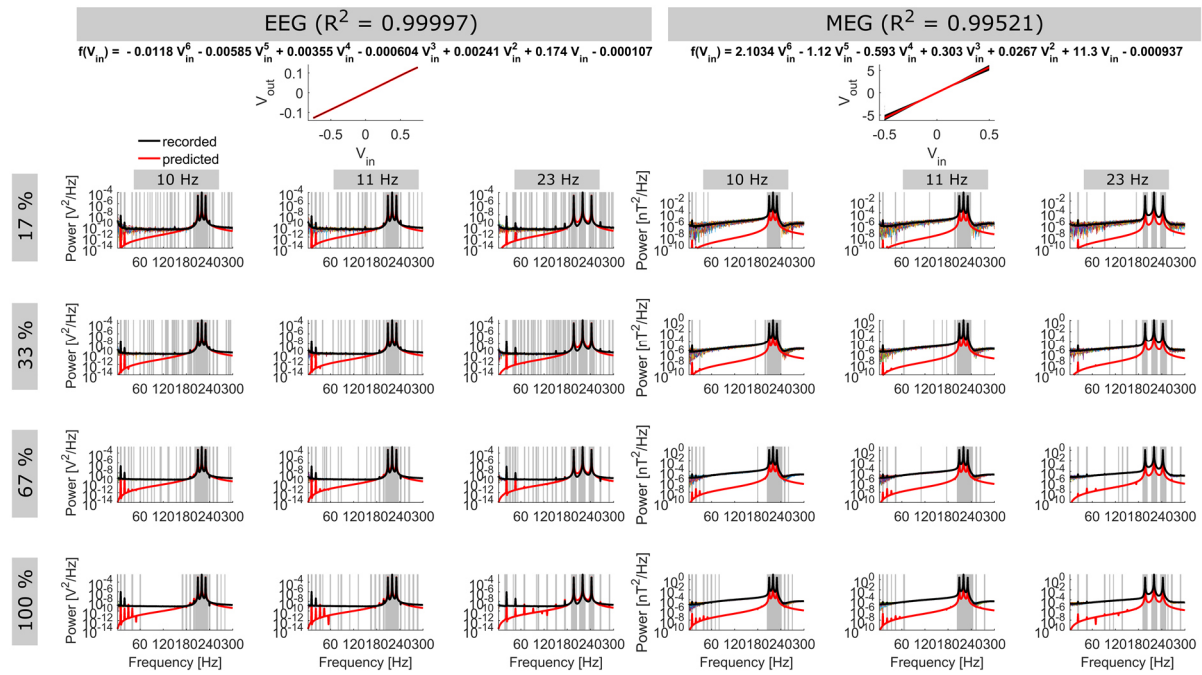
483 **Highlights**

- 484 • Amplitude modulated tACS generates spurious artifacts at its modulation frequency
- 485 • The input-output transfer functions of different AM-tACS setups was estimated
- 486 • Hardwares non-linear transfer characteristics account for these spurious artifacts
- 487 • An analysis approach to characterize non-linearities of tACS setups is provided.

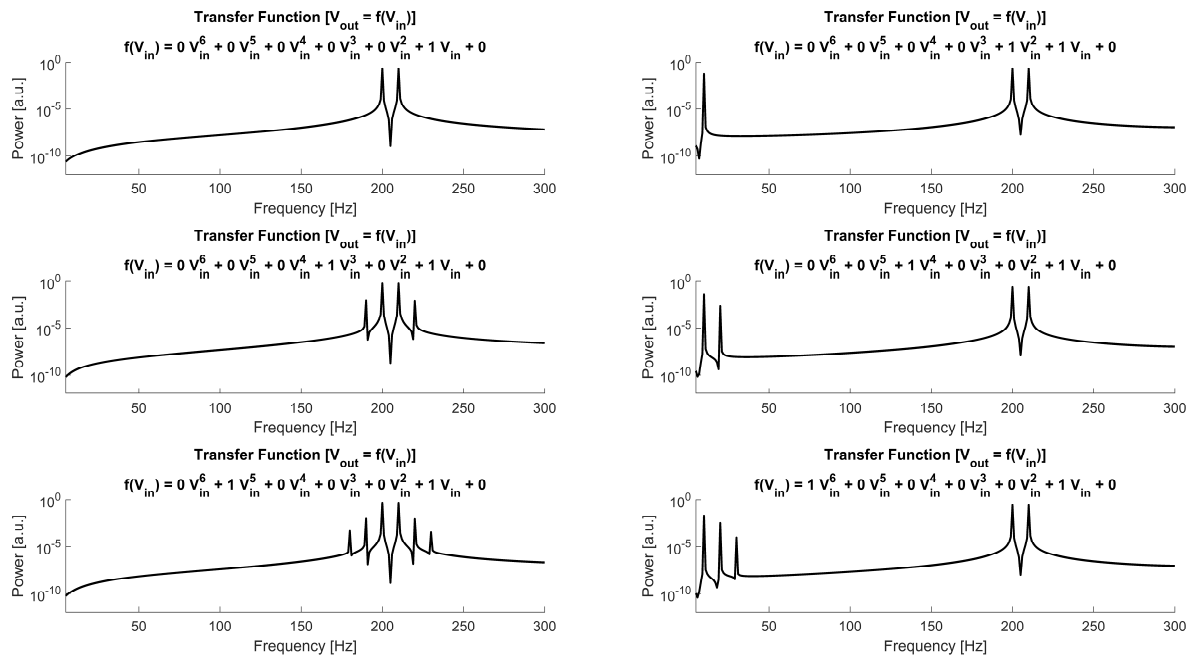
488 **Supplementary Materials: Non-linear transfer characteristics of**
 489 **stimulation and recording hardware account for spurious low-**
 490 **frequency artifacts during amplitude modulated transcranial al-**
 491 **ternating current stimulation (AM-tACS)**



492
 493 **Supplementary Figure S1: Full range version of Figure 2.** TFs (top) show recorded probe
 494 stimulus amplitudes in relation to their input amplitudes (V_{out}/V_{in} ; black dots), as well as the
 495 course of the TF model (red line). The corresponding function is displayed in the title. Spectra
 496 show average power at each frequency in the different AM-recordings (black line). Thin colored
 497 lines show power spectra for each of the 60 repetitions. Red line shows the spectrum predicted
 498 by evaluating the digital AM-signal by the estimated TF of the setup. Grey areas indicate fre-
 499 quencies significantly differing in power compared to the two neighboring frequencies ($p < .05$,
 500 bonferroni corrected). Please note the different scaling of the power spectra.



Supplementary Figure S2: Full range version of Figure 3. TFs (top) show recorded probe stimulus amplitudes in relation to their input amplitudes (V_{out}/V_{in} ; black dots), as well as the course of the TF model (red line). The corresponding function is displayed in the title. Spectra show average power at each frequency in the different AM-recordings (black line). Thin colored lines show power spectra for each of the 60 repetitions. Red line shows the spectrum predicted by evaluating the digital AM-signal by the estimated TF of the setup. Grey areas indicate frequencies significantly differing in power compared to the two neighboring frequencies ($p < .05$, bonferroni corrected). Please note the different scaling of the power spectra.



510

511 **Supplementary Figure S3: Simulation of artifacts resulting from temporal interference**

512 **(TI)**. Frequency spectra showing the effect of non-linear TF terms on amplitude modulated
 513 signals created by TI. Similar to the am-signals, the TI signals contain no low-frequency artifact
 514 when a solely linear TF is applied (**top left**). Adding non-linear terms to the TF model results
 515 in additional side-bands around the frequencies of the two applied sine wave signals for odd-
 516 valued exponents (**left column**) and in low-frequency artifacts at Δf (corresponding to the
 517 modulation frequency of the am-signal generated by the TI signals) and its harmonics for even
 518 valued exponents of the TF model (**right column**).